

Fabrication of Supported Cuprous Sites at Low Temperatures: An Efficient, Controllable Strategy Using Vapor-Induced Reduction

Wen-Juan Jiang, Yu Yin, Xiao-Qin Liu,* Xiao-Qian Yin, Yao-Qi Shi, and Lin-Bing Sun*

State Key Laboratory of Materials-Oriented Chemical Engineering, College of Chemistry and Chemical Engineering, Nanjing University of Technology, Nanjing 210009, China

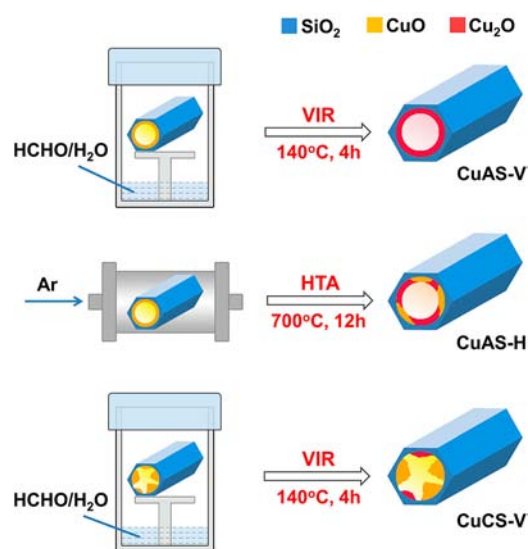
S Supporting Information

ABSTRACT: Selective reduction of supported CuO to Cu₂O was realized using the strategy of vapor-induced reduction, in which HCHO/H₂O vapor diffuses into the pores of the support and interacts with predispersed CuO. This new strategy allows the fabrication of supported cuprous sites at much lower temperatures within a short time, avoids the formation of Cu(0) with a Cu(I) yield of nearly 100%, and results in materials with good adsorption performance, which is impossible to achieve by conventional methods.

Because of its versatility, nontoxicity, and low cost, cuprous oxide (Cu₂O) is highly promising for diverse applications such as adsorption, photocatalysis, and sensing.¹ Much attention has therefore been given to the fabrication of cuprous sites on various supports, including alumina, silica, zeolite, and metal–organic frameworks.² To obtain cuprous sites, the precursor, usually cupric oxide (CuO), is introduced into the support by decomposition of a copper salt. For the fabrication of Cu₂O-containing functional materials, the subsequent conversion of the supported cupric sites to cuprous ones is considered a crucial step. To date, two approaches have been employed: (i) thermal treatment at ~200 °C in the presence of a reducing gas (e.g., H₂ or CO) and (ii) high-temperature autoreduction (HTA) under an inert atmosphere. Only a few reports concern the use of the first approach, since the reduction process is hard to control and Cu(0) rather than Cu(I) is frequently produced, as has been well-demonstrated by H₂ temperature-programmed reduction (H₂-TPR) results in a large number of studies.³ The second approach involving HTA can avoid the formation of Cu(0) and has been widely utilized for the preparation of Cu(I)-containing materials.⁴ However, it requires high temperatures (>700 °C) and long treatment times (>12 h), which are energy-consuming and harmful to the structure of the material. Moreover, only about half of the CuO can be converted to Cu₂O using the HTA approach, which is far from satisfactory.⁵ Hence, the development of an efficient, controllable method to construct supported cuprous sites is extremely desirable.

Herein we report for the first time a strategy for constructing cuprous sites on SBA-15 mesoporous silica by using vapor-induced reduction (VIR) (Scheme 1). A formaldehyde/water vapor mixture generated at elevated temperatures diffuses into the pores of SBA-15 and interacts with predispersed CuO, leading to the formation of Cu₂O. This strategy allows the

Scheme 1. Conversion of Dispersed or Aggregated CuO to Cu₂O on Mesoporous Silica by the VIR and HTA Approaches



reduction of CuO at temperatures as low as 140 °C, which is significantly lower than the HTA method (700 °C). More importantly, almost all of the CuO can be converted, and the yield of Cu₂O is nearly 100%. The present strategy offers an efficient and controllable way to fabricate supported cuprous sites under mild conditions, which is impossible to realize by conventional methods. We also demonstrate that the VIR-treated samples exhibited excellent performance in the adsorptive separation of ethylene and ethane that was obviously superior to the results using samples prepared by the HTA method.

Two types of CuO-containing SBA-15 precursors, namely, CuAS and CuCS, were first synthesized by using as-prepared and calcined SBA-15, respectively [see the Supporting Information (SI) for experimental details].⁵ After the introduction of CuO, the ordered mesostructure was well-preserved, as shown by low-angle X-ray diffraction (XRD) and N₂ adsorption results (Figures S1 and S2 and Table S1 in the SI). A great difference between the two types of samples was the degree of dispersion of CuO. All of the CuO was well-dispersed in the CuAS samples as a result of the confining effect

Received: March 26, 2013

Published: May 16, 2013

of as-prepared SBA-15 in the synthetic process, while aggregation of CuO occurred in CuCS, as demonstrated by diffraction lines in wide-angle XRD patterns (Figure S1).⁶ In contrast to the aggregated CuO, the reduction temperature of dispersed CuO was obviously lower, as shown in the H₂-TPR profiles (Figure S3). Hence, all of the CuAS samples exhibited a much lower temperature for CuO reduction than the sample CuCS(4) (where the value in parentheses indicates the Cu content in mmol/g). It was noticeable that only one H₂ consumption peak was observed for all of the samples, and the amount of H₂ consumed was in good agreement with the CuO content (Table S1). This suggests that supported CuO, regardless of the degree of dispersion, is directly reduced to metallic Cu in the presence of reducing gases.

Treatment of CuAS and CuCS using the VIR strategy resulted in the formation of CuAS-V and CuCS-V, respectively. For comparison, CuAS-H was also prepared by treatment of CuAS with the HTA method (Scheme 1). All of the CuAS-V samples showed an intense diffraction line accompanied by two weak ones in the low-angle XRD patterns (Figures 1A and S4),

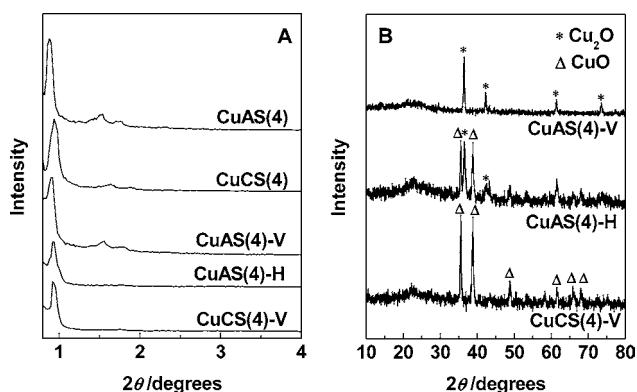


Figure 1. (A) Low-angle and (B) wide-angle XRD patterns of various samples.

which can be indexed as the (100), (110), and (200) reflections corresponding to the two-dimensional hexagonal pore regularity of the *p6mm* space group. These reflections, in combination with the transmission electron microscopy images shown in Figure S5, provide evidence of the good maintenance of mesostructure after reduction. Comparison of the samples before and after reduction showed that the intensity of the diffraction peaks of CuAS(4) was comparable to that of CuAS(4)-V. In the case of CuAS(4)-H and CuCS(4)-V, however, the (100) peak became weaker and the (110) and (200) peaks disappeared. The N₂ adsorption/desorption isotherms of the CuAS-V samples were of type IV with an H1 hysteresis loop, which is characteristic of materials with cylindrical mesopores (Figure S6). Further calculation revealed that the surface areas and pore volumes decreased progressively with increasing Cu content (Table S2). The sample CuAS(4)-V had a surface area of 400 m²/g and a pore volume of 0.768 cm³/g, which are apparently larger than those of CuAS(4)-H and CuCS(4)-V containing the same amount of Cu. On the basis of the above results, it is safe to say that the CuAS-V samples possessed better mesostructure than CuAS-H and CuCS-V.

The diffraction peaks in the wide-angle XRD pattern of CuAS-V were well-consistent with those of Cu₂O (JCPDS no. 65-3288; Figures 1 and S4), indicating the efficiency of the VIR

strategy in the controllable reduction of CuO. However, it was hard to identify any diffraction peaks originating from Cu₂O in the pattern for CuCS(4)-V, and peaks ascribed to CuO (JCPDS no. 48-1548) became predominant. This means that the reduction of aggregated CuO is much more difficult than that of dispersed CuO. Interestingly, the crystalline phases of CuO and Cu₂O with comparable peak intensities coexisted in CuAS(4)-H. It is apparent that only part of the CuO was converted to Cu₂O using the HTA method, even though CuO was well-dispersed in the precursor.

The H₂-TPR profiles shown in Figures 2 and S7 present interesting results on the reduction of different samples

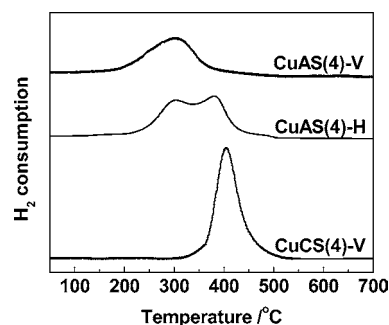


Figure 2. H₂-TPR profiles for the CuAS-V, CuAS-H, and CuCS-V samples.

prepared using the VIR and HTA methods. All of the CuAS-V samples exhibited a single peak of H₂ consumption at ~300 °C. On the basis of the aforementioned XRD results, this peak can be tentatively assigned to the transformation of Cu(I) to Cu(0). The amounts of consumed H₂ calculated from the peak areas provide further evidence of this assignment (Tables 1 and

Table 1. H₂ Consumption and Amount of Copper in Different Samples

sample	Cu content ^a (mmol/g)	H ₂ consumed ^b (mmol/g)	Amount of Cu(I) ^c (mmol/g)	Cu(I) yield (%) Cu(I)/[Cu(I)+Cu(II)]	
				from H ₂ consumed ^d	from titration ^e
CuAS(4)-V	4.0	2.01	3.98	99.5	99.6
CuAS(4)-H	4.0	2.85	2.30	57.5	57.9
CuCS(4)-V	4.0	3.94	0.12	3.0	3.1

^aAmount of Cu introduced into SBA-15. ^bCalculated from the H₂-TPR results. ^cDetermined by titration. ^dCalculated from the amount of H₂ consumed and the total Cu content. ^eCalculated from the titration results and the total Cu content.

S3). For CuAS(4)-V with a Cu content of 4 mmol/g, the amount of H₂ consumed was 2.01 mmol/g. It is therefore clear that Cu(I) rather than Cu(II) was predominant in CuAS(4)-V, as otherwise the amount of H₂ consumed would have been much larger. Titration results showed that the amount of Cu(I) in CuAS(4)-V was 3.98 mmol/g. Calculations of the Cu(I) yield in CuAS(4)-V based on the amount of H₂ consumed and the titration data gave values of 99.5% and 99.6%, respectively. These results thus demonstrate that the VIR strategy can effectively reduce dispersed CuO to Cu₂O with high selectivity. The UV-vis technique was also introduced to characterize the samples before and after reduction. As shown in Figure S8, the

UV-vis spectra of CuAS(4) and CuAS(5) presented two absorption peaks at ~ 270 and ~ 760 nm, which can be assigned to CuO.⁷ For the samples after reduction, namely, CuAS(4)-V and CuAS(5)-V, the peaks at 270 and 760 nm were absent, while a new peak at 450 nm originated from Cu₂O emerged.⁸ The UV-vis data thus confirm the results described above, pointing out the complete conversion of dispersed CuO to Cu₂O using the VIR strategy. In contrast to dispersed CuO, aggregated CuO was quite difficult to convert to Cu₂O under the same conditions. The CuCS(4)-V sample gave a peak of H₂ consumption at ~ 400 °C, and the amount of H₂ consumed was calculated to be 3.94 mmol/g. Further calculations showed that the yield of Cu(I) was 3.0%, which is in line with the titration result (3.1%). Apparently, only a tiny amount of CuO in CuCS(4) was converted to Cu₂O, while CuO became more aggregated in the VIR process. This led to an increase in the reduction temperature in the H₂-TPR profiles, as can be seen by comparing the profiles for the samples before and after treatment (Figures 2 and S3). Two reduction peaks were observed for CuAS(4)-H because of the coexistence of CuO and Cu₂O. A medium amount of H₂ was consumed (2.85 mmol/g), corresponding to a Cu(I) yield of 57.5%. Such a yield is evidently lower than that for the same sample prepared using the VIR strategy ($\sim 100\%$), despite the much higher temperature and longer time demanded for the HTA process.

Our materials were also applied to the adsorptive separation of C₂H₄ and C₂H₆. C₂H₄ is an important chemical with versatile applications. Conventionally, C₂H₄/C₂H₆ separation is carried out by distillation at -25 °C and 2000 kPa, which is one of the most energy-intensive processes in the chemical industry.⁹ Extensive attention has recently been paid to the separation of C₂H₄ and C₂H₆ by adsorption, as this process can be performed under mild conditions.¹⁰ Among various alternatives, supported Cu₂O is a good choice of adsorbent because of its low cost, high activity, and good reusability. The adsorption isotherms in Figure 3 show that CuCS(4)-V adsorbed 1.75 mmol of C₂H₄/g at 1000 kPa, which is close

to the uptake of C₂H₆ (1.59 mmol/g). Under the same conditions, the C₂H₄ uptake increased to 2.23 and 2.63 mmol/g on CuAS(4)-H and CuAS(4)-V, respectively, while the C₂H₆ uptake remained almost constant. To provide a better understanding of the adsorption behavior, the C₂H₄/C₂H₆ selectivity was predicted using ideal adsorbed solution theory (IAST), and the results are presented in Figure 3D. The C₂H₄/C₂H₆ selectivities of the different adsorbents decreased in the order CuAS(4)-V > CuAS(4)-H > CuCS(4)-V, despite different molar fractions of the two adsorbates. To take one example, the C₂H₄/C₂H₆ selectivity was 1.7 on CuCS(4)-V at a C₂H₄ molar fraction of 0.2. A selectivity of 5.9 was obtained on CuAS(4)-H, and the selectivity was as high as 10.3 on CuAS(4)-V. Among CuAS-V samples with different Cu contents, CuAS(4)-V exhibited the best performance with regard to C₂H₄/C₂H₆ separation (Figures S9 and S10). After adsorption, regeneration of the spent CuAS(4)-V adsorbent was also conducted (Figure S11). The adsorptive capacity of the regenerated adsorbent could be well-recovered upon recycling three times. It is known that cuprous species can interact with the C=C bond in C₂H₄ through π -complexation, which gives rise to preferential adsorption of C₂H₄ over C₂H₆.¹¹ As a result, the content of Cu(I) in the adsorbent plays a significant role in C₂H₄/C₂H₆ separation. Of course, some other factors such as surface area and pore volume must also be taken into consideration.

To examine the pathway for reduction, a CuAS sample treated using the VIR strategy for different times was monitored by XRD. As depicted in Figure S12, no diffraction lines were observed for the sample before treatment because CuO was well-dispersed in the pores of SBA-15. A new diffraction line derived from Cu(OH)₂·H₂O (JCPDS no. 42-0746) emerged at 1 h and disappeared at 4 h, indicating that Cu(OH)₂·H₂O is an intermediate in the reduction process. The diffraction lines of Cu₂O appeared at 2 h, and their intensity increased with increasing reaction time, corresponding to increases in the amount of Cu₂O. In terms of these investigations, the reduction pathway shown in eqs 1–3 can be proposed:

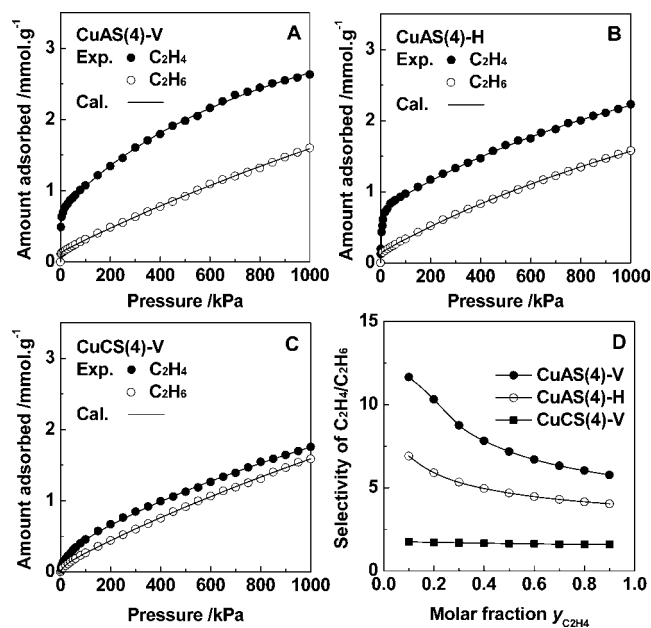
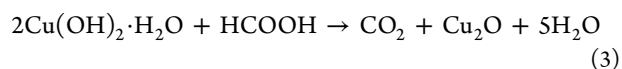
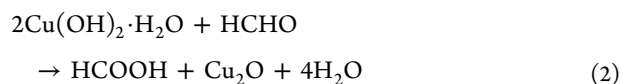
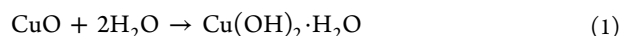


Figure 3. (A–C) Adsorption isotherms of C₂H₄ and C₂H₆ over different samples. (D) C₂H₄/C₂H₆ selectivity.

Driven by the concentration gradient, HCHO goes into the gas phase from solution at elevated temperatures and subsequently diffuses into the pores of the mesoporous silica. The reduction reaction between HCHO and the intermediate then takes place, leading to the formation of Cu₂O and formic acid (HCOOH). In view of the reducing ability of HCOOH, the transformation of the intermediate to Cu₂O continues, accompanied by the formation of CO₂. Gas chromatography analysis indicated the presence of both HCOOH and CO₂ in the reaction mixture, thus confirming the pathway. For CuAS and CuCS samples containing identical amounts of CuO, quite different reduction behavior was observed in the VIR process. Apparently, the degree of dispersion of CuO has an important effect on the reduction. We consider that dispersed CuO, which is easily accessed by gaseous HCHO, is more readily reduced.

Hence, the reduction efficiency is strongly dependent on the degree of dispersion of CuO.

Despite great efforts, the development of an efficient method to fabricate supported cuprous sites has remained a challenge until now. In the traditional HTA method, precursors have to be treated at high temperatures (>700 °C) for quite a long time (>12 h), which is time- and energy- consuming. The present VIR strategy allows the reduction of supported cupric species to cuprous sites at temperatures as low as 140 °C, and the whole process can be completed within 4 h, which evidently saves a great deal of time and energy. More importantly, the yield of Cu₂O is nearly 100%, without the formation of metallic Cu. Our strategy provides an efficient and controllable way to construct cuprous active sites, which is highly desired in the fields of adsorption, catalysis, sensing, and so on. Furthermore, this novel strategy should enable us to introduce various metal oxides and even metals into porous materials with a range of pore symmetries and pore sizes, which is impossible or difficult to accomplish by conventional methods.

■ ASSOCIATED CONTENT

■ Supporting Information

Experimental details and additional data. This material is available free of charge via the Internet at <http://pubs.acs.org>.

■ AUTHOR INFORMATION

Corresponding Author

liuxq@njut.edu.cn; lbsun@njut.edu.cn

Notes

The authors declare no competing financial interest.

■ ACKNOWLEDGMENTS

We acknowledge financial support of this work by the National Natural Science Foundation of China (21006048 and 20976082), the Specialized Research Fund for the Doctoral Program of Higher Education of China (20093221120001), the China Postdoctoral Science Foundation (20110491406), Jiangsu Planned Projects for Postdoctoral Research Funds (1101155C), the Research and Innovation Project for College Graduates of Jiangsu Province (CXZZ11_0350 and CXZZ12_0432), and the Priority Academic Program Development of Jiangsu Higher Education Institutions.

■ REFERENCES

- (1) (a) Deng, S.; Tjoa, V.; Fan, H. M.; Tan, H. R.; Sayle, D. C.; Olivo, M.; Mhaisalkar, S.; Wei, J.; Sow, C. H. *J. Am. Chem. Soc.* **2012**, *134*, 4905. (b) Huang, W.-C.; Lyu, L.-M.; Yang, Y.-C.; Huang, M. H. *J. Am. Chem. Soc.* **2011**, *134*, 1261. (c) Sui, Y.; Fu, W.; Zeng, Y.; Yang, H.; Zhang, Y.; Chen, H.; Li, Y.; Li, M.; Zou, G. *Angew. Chem., Int. Ed.* **2010**, *49*, 4282. (d) Kuo, C.-H.; Yang, Y.-C.; Gwo, S.; Huang, M. H. *J. Am. Chem. Soc.* **2011**, *133*, 1052. (e) He, G.-S.; Sun, L.-B.; Song, X.-L.; Liu, X.-Q.; Yin, Y.; Wang, Y.-C. *Energy Fuels* **2011**, *25*, 3506. (f) Hung, L. I.; Tsung, C. K.; Huang, W. Y.; Yang, P. D. *Adv. Mater.* **2010**, *22*, 1910. (g) Zuo, J. M.; Kim, M.; O'Keeffe, M.; Spence, J. C. H. *Nature* **1999**, *401*, 49.
- (2) (a) Fei, H.; Rogow, D. L.; Oliver, S. R. *J. Am. Chem. Soc.* **2010**, *132*, 7202. (b) White, B.; Yin, M.; Hall, A.; Le, D.; Stolbov, S.; Rahman, T.; Turro, N.; O'Brien, S. *Nano Lett.* **2006**, *6*, 2095. (c) Hernández-Maldonado, A. J.; Yang, F. H.; Qi, G.; Yang, R. T. *Appl. Catal., B* **2005**, *56*, 111. (d) Hernández-Maldonado, A. J.; Qi, G.; Yang, R. T. *Appl. Catal., B* **2005**, *61*, 212. (e) Khan, N. A.; Jhung, S. H. *Angew. Chem., Int. Ed.* **2012**, *51*, 1198. (f) Khan, N. A.; Jhung, S. H. *J. Hazard. Mater.* **2012**, *237–238*, 180. (g) Song, X.-L.; Sun, L.-B.; He,

G.-S.; Liu, X.-Q. *Chem. Commun.* **2011**, *47*, 650. (h) Yang, R. T.; Hernández-Maldonado, A. J.; Yang, F. H. *Science* **2003**, *301*, 79.

(3) (a) Bridier, B.; Pérez-Ramírez, J. *J. Am. Chem. Soc.* **2010**, *132*, 4321. (b) Kim, J. Y.; Rodríguez, J. A.; Hanson, J. C.; Frenkel, A. I.; Lee, P. L. *J. Am. Chem. Soc.* **2003**, *125*, 10684. (c) Kaminski, P.; Sobczak, I.; Decyk, P.; Ziolk, M.; Roth, W. J.; Campo, B.; Daturi, M. *J. Phys. Chem. C* **2013**, *117*, 2147.

(4) Wang, Y.; Yang, R. T.; Heinzl, J. M. *Ind. Eng. Chem. Res.* **2009**, *48*, 142.

(5) Tian, W.-H.; Sun, L.-B.; Song, X.-L.; Liu, X.-Q.; Yin, Y.; He, G.-S. *Langmuir* **2010**, *26*, 17398.

(6) Yin, Y.; Jiang, W.-J.; Liu, X.-Q.; Li, Y.-H.; Sun, L.-B. *J. Mater. Chem.* **2012**, *22*, 18514.

(7) (a) Liu, Z. L.; Amiridis, M. D.; Chen, Y. *J. Phys. Chem. B* **2005**, *109*, 1251. (b) Velu, S.; Suzuki, K.; Okazaki, M.; Kapoor, M. P.; Osaki, T.; Ohashi, F. *J. Catal.* **2000**, *194*, 373.

(8) Zhang, S.; Zhang, S.; Peng, F.; Zhang, H.; Liu, H.; Zhao, H. *Electrochem. Commun.* **2011**, *13*, 861.

(9) (a) Yang, R.; Kikkinides, E. *AIChE J.* **1995**, *41*, 509. (b) Ruthven, D. M.; Reyes, S. C. *Microporous Mesoporous Mater.* **2007**, *104*, 59.

(10) (a) Aguado, S.; Bergeret, G.; Daniel, C.; Farrusseng, D. *J. Am. Chem. Soc.* **2012**, *134*, 14635. (b) Albesa, A. G.; Rafti, M.; Rawat, D. S.; Vicente, J. L.; Migone, A. D. *Langmuir* **2012**, *28*, 1824. (c) Bao, Z.; Alnemrat, S.; Yu, L.; Vasiliev, I.; Ren, Q.; Lu, X.; Deng, S. *Langmuir* **2011**, *27*, 13554. (d) Bloch, E. D.; Queen, W. L.; Krishna, R.; Zadrozny, J. M.; Brown, C. M.; Long, J. R. *Science* **2012**, *335*, 1606.

(11) (a) Jiang, W.-J.; Sun, L.-B.; Yin, Y.; Song, X.-L.; Liu, X.-Q. *Sep. Sci. Technol.* **2013**, *48*, 968. (b) Takahashi, A.; Yang, R. T.; Munson, C. L.; Chinn, D. *Langmuir* **2001**, *17*, 8405.